Indian Journal of Chemistry
Vol. 61, November 2022, pp. 1216-1223
DOI: 10.56042/ijc.v61i11.68275

DFT Analysis, ADME, antibacterial activity and molecular docking studies of 2-(3-aryl-1,2,4-oxadiazol-5-yl)-n-phenylacetamide derivatives

Susmitha Kasula[a], Srivani Kandukoori[b], Laxminarayana Eppakayala[c] & Thirumala Chary Maringanti[d,*]

[a]Department of Chemistry, St. Francis College for Women, Begumpet, Hyderabad- 500 016, India

[b]Lal Bahadur College, Post Graduate Centre, Mulugu Cross road, Nizampura, Warangal-506 002, India

[c]Sreenidhi Institute of Science and Technology (Autonomous) Yamnampet, Ghatkesar, Hyderabad, India

[d]Jawaharlal Nehru Technological University, Kukatpally, Hyderabad-500 085, India

*E-mail: mtcharya@yahoo.com

Received 11 July 2021; accepted (revised) 17 October 2022

Quantum computational study based on density functional theory (DFT/B3LYP) using basis set 6-311G (d,p) a number of global and local reactivity descriptors have been computed to predict the reactivity and the reactive sites on the 2-(3-aryl-1,2,4-oxadiazol-5-yl)-n-phenylacetamideoxadiazole derivatives. The molecular geometry and the electronic properties such as frontier molecular orbital (HOMO and LUMO), ionization potential (I) and electron affinity (A) are investigated to get a better insight of the molecular properties. Molecular electrostatic potential (MEP) for all compounds were determined to check their electrophilic or nucleophilic reactivity. The *in silico* pharmacokinetics showed that nearly all derivatives obeyed Lipinski rule of 5 with low toxicity and metabolic stability. The antibacterial activity was carried out against *B. subtilis,* S. *aureus, P.aeruginosa* and E. *coli*, displaying considerable inhibition. MurE ligases, (PDB: 7b6k) participating in the intracellular steps of bacterial peptidoglycan biosynthesis, are taken as targets for molecular docking studies using Flare GUI software. The docking outcome revealed that these 1,2,4-oxadiazole analogues have highest LF rank score in the range -12.9 to -6.0 which shows that they act as potent antibacterial agents.

Keywords: 1,2,4-oxadiazole,DFT, Molecular Docking, MurE ligases(PDB ID: 7b6k)

Heterocyclic products have attracted interest of researchers due to their various medicinal standards. Oxadiazoles comes under five-membered heterocyclic compounds carrying two nitrogen and one oxygen atom[1]. From previous literature 1,2,4-oxadiazole scaffold has been broadly investigated for various biological activities covering anti-inflammatory[2,3], analgesic[4], anaesthetic[5], anthelmintic[6], antiallergic[7], anti-Alzheimer[8], anti-bacterial[9,10] anticancer[11-13], anticonvulsant[14,15], antidepressant[16], antifungal[17], anti-HIV[18], antiparasitic[19]and anti-tubercular activities[20]. Recently we reported a simple and efficient method of synthesis 2-(3-aryl-1,2,4-oxadiazol-5-yl)-N-phenylacetamide derivatives using acid chlorides from 3-(hydroxyimino)3-amino-N-phenylpropanamide[21].

Reactivity in chemistry is a crucial concept because it is intimately associated with reaction mechanisms thus allowing understanding chemical reactions and developing synthesis methods to obtain new materials. A branch of Density Functional Theory (DFT) [22] called Conceptual DFT has been developed to calculate, a set of global and local descriptors which are used to measure the reactivity of molecular systems[23]. Due to the diverse biological importance of 1,2,4-oxadiazole analogs a detailed structure-chemical reactivity relations have been accepted. The present paper gives a complete description of the molecular geometry, global and local reactivity descriptors, and MEP features of the title compounds. All DFT calculations are carried out at B3LYP 6-311G (d,p) basis set by using spartan 18 parallel suite software. Further, toxicity screening (using PreAdmet Server) evaluation of their antibacterial activity supported with molecular docking studies (using FLARE GUI Software) were carried out with MurE ligases, (PDB: 7b6k) as target enzyme.

Experimental Details

The synthesized derivatives of 2-[3-(phenyl)-[1,2,4] oxadiazol-5-yl]-N-phenyl-acetamide (3a – g) (Scheme. 1) were screened via *in silico* calculations, i.e., pharmacokinetic limits including ADME, DFT (frontier orbital calculations) and molecular docking study. Further, they were subjected to antibacterial studies.

In silico DFT calculation

The chemical reactivity and global reactivity descriptors for the 2-[3-(phenyl)-[1,2,4]oxadiazol-5-yl]-N-phenyl-acetamide derivatives were calculated using DFT study at B3LYP/6-311G(d,p) level of computation using sspartan 18 parallel suite software.

Calculation of pharmacokinetic and toxicity parameters

The molecular characteristics of synthesized compounds 3a–g was calculated using the FLARE GUI software. Number of atoms, molecular weight, partition coefficient (Log P), topo-logical surface area (TPSA), hydrogen bond donors and acceptors, and Lipinski's rule violations were calculated to assess drug likeliness. Pre-ADMET web server version 2.0 was used to calculate ADME features (adsorption, distribution, metabolism, and excretion). To measure oral absorption, the ADME parameters include plasma protein binding (PPB), human intestinal absorption (HIA), logKp (degree of skin permeability), Caco2 cell lines, and MDCK cell lines**.**

Antibacterial studies

The antibacterial activity of the newly synthesized compounds was tested against *Bacillus substilis*, *Staphylococcus aureus*, *Escherichia coli* and *Pseudomonas aeruginosa*. The antibacterial effectiveness was determined using the disc diffusion method[24,25]. Each labelled petri dish received 20 mL of sterile nutritional agar material, which was then solidified. On the surface, a freshly prepared bacterial inoculum was dispersed. As a positive control, gentamycin was used. All Petri dishes were incubated for 24–48 hours at 37°C. The diameter of the zone of inhibition against the test substance was measured and the results were recorded.

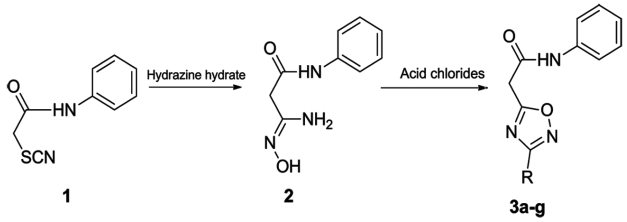

Scheme 1 — Synthetic protocol for 2-[3-(phenyl)-[1,2,4] oxadiazol-5-yl]-N-phenyl-acetamide derivatives (3a – g)

In-silico molecular docking studies

Molecular docking studies were performed for synthesized derivatives 2-[3-(phenyl)-[1,2,4] oxadiazol-5-yl]-N-phenyl-acetamide by using Flare GUI SOFTWARE. It was worthwhile to conduct *in silico* studies to predict the binding affinity and orientation at the active site of the protein in connection to in-vitro antibacterial activity. The structure of synthesized compounds was depicted in Marvin sketch with suitable 2-D orientation and structural drawing errors were checked. With the least amount of energy, a two-dimensional structure was turned into a three-dimensional representation. The ligand molecules with the lowest energy were used as input for the Flare GUI SOFTWARE, which is ideal for molecular docking research. MurE ligases participating in the intracellular steps of bacterial peptidoglycan biosynthesis was chosen as the target macromolecule. As a receptor molecule, the PDB coordinate file (7b6k) was used. Water molecules and other interfering groups were removed from the receptor molecule, and the side chain of the receptor was rebuilt by using Freed Build Loop within Flare GUI python extensions. The final visual portrayal of binding interactions between ligand and target macromolecule/protein was shown by using Discovery Studio software.

Results and Discussion

Pharmacokinetic and ADME parameters

Lipinski's rule of five (MW 500, Log P <5, number of H bond donors up to 5 and H bond acceptors up to 10 shown in Table 1 fit all of the compounds well with drug like behaviour. Table 2 shows the

Table 1 — Drug likeliness properties of 1,2,4 oxadiazol derivatives (3a–g)

Name	Mol.Wt. (amu)	Dipole (D)	HBD Count	HBA Count	Polarizability	WLOGP	SlogP	TPSA	Lipinski #violations	#RB
3a	279.299	3.86	1	5	63.21	3.38	3	68	0	4
3b	313.744	2.06	1	5	64.35	2.73	2.3	68	0	4
3c	313.744	3.53	1	5	64.36	3.38	3	68	0	4
3d	297.289	2.45	1	5	63.58	3.29	2.8	68	0	4
3e	297.289	3.52	1	5	63.61	3.29	2.8	68	0	4
3f	309.325	3.22	1	6	65.4	2.74	2.4	77.3	0	5
3g	309.325	5.03	1	6	65.36	2.74	2.4	77.3	0	5

Table 2 — ADME Properties of 1,2,4 oxadiazol derivatives (3a–g)

ID	3a	3b	3c	3d	3e	3f	3g
BBB	0.73	0.38	0.41	0.56	0.34	0.64	0.034
Caco2	13.53	21.79	21.79	16.32	16.32	11.24	14.01
HIA	96.09	96.04	96.04	96.09	96.09	96.56	96.56
MDCK	45.98	21.23	14.70	38.59	31.25	37.33	35.06
PPB	100	93.16	98.69	95.96	97.37	97.89	98.91
SP	-3.27	-3.31	-3.30	-3.56	-3.55	-3.43	-3.43

*BBB: Blood Brain Barrier. *HIA: Human Intestinal Absorption. *PPB: Plasma Protein Binding. *SP: Skin Permeability.

Table 3 — Toxicity profilesof 1,2,4 oxadiazole derivatives (3a–g)

ID	3a	3b	3c	3d	3e	3f	3g
Acute algae toxicity	0.0643	0.0320	0.0328	0.0506	0.0506	0.0515	0.0511
mutagenicity	mutagen	mutagen	mutagen	mutagen	mutagen	mutagen	Mutagen
Carcinogenicity (Mouse)	negative	negative	negative	positive	positive	negative	Negative
Carcinogenicity (Rat)	negative	negative	negative	negative	negative	negative	Negative
Acute daphina toxicity	0.1080	0.0414	0.0464	0.0846	0.0889	0.1021	0.1009
hERG_ inhibition	low_risk	Medium_risk	Medium risk	Medium risk	Medium risk	Medium risk	Medium Risk
Acute fish toxicity (medaka)	0.0201	0.0034	0.0042	0.0125	0.0138	0.0185	0.0181
Acute fish toxicity (minnow)_	0.037684	0.010788	0.010754	0.017638	0.0175301	0.0373974	0.0374049

ADME characteristics that predicted favorable pharmacokinetics and bioavailability. The fact that the HIA values were above 90% suggested that the compounds were well absorbed orally. The low Kp values suggested inadequate skin permeability, which led to high oral.There will be no effect if the product comes into touch with the skin by accident. The PPB values were less than 100%.Caco 2 readings in the range of 4-25 were considered moderately permeable. Except for 3b , 3c, MDCK values greater than 25 indicated good absorption. All of the compounds (Table 2) were chosen after passing the Wlogp<5 and TPSA <75. The boiled egg model using swiss ADME is offered as a precise predictive model that works by computing tiny molecule lipophilicity and polarity[26]. The WLOGP-versus-TPSA of the compounds (Fig. 1) revealed that they are all highly absorbable across the blood-brain barrier. Predictions using preADMET, on the other hand, revealed that except two compounds3d, 3e all showed negative carcinogenicity to mouse but mutagenic. All have a modest risk of cardiotoxicity, according to the hERG inhibition prediction Table 3.

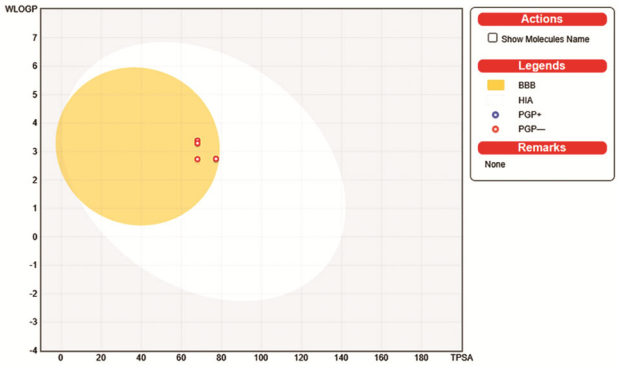

Fig. 1 — Water partition coefficient (WlogP) vs. topological polar surface area (TPSA) in a boiled egg figure, indicating the highest possibility of permeation to the brain

Frontier orbital calculation

The molecule's interaction with other species is determined by the Frontier molecular orbital theory. HOMO (highest occupied orbital), which is assumed to be the outermost orbital containing electrons, tends to act as an electron donor. LUMO (lowest unoccupied molecular orbital) on the other hand, can be thought of as the innermost orbital with free locations to accept electrons[27]. The energy gap is the difference in energy between the HOMO and LUMO orbitals. LUMO aids in the identification of a molecule's chemical reactivity and kinetic stability [28 -30]. A polarized molecule with a small gap is classified as a soft molecule with strong chemical reactivity. Table 4 shows the energies of the HOMO and LUMO of some of the 1, 2, 4 oxadiazole derivatives (Fig. 2) determined using the DFT method at the B3LYP 6-311G (d,p) basis set. Furthermore, HOMO and LUMO are critical quantum chemical parameters for determining a molecule's reactivity and are utilized to determine a variety of important metrics such as chemical reactivity descriptors. The amount of energy required to remove an electron from a molecule is

Table 4 — Electronic energy (eV) calculation values of 1,2,4 oxadiazole synthesis scheme

Name	E_{HOMO}	E_{LUMO}	Band gap (ΔE)
1	-6.64	-1.49	5.15
2	-6.1	-0.5	5.6
3a	-6.29	-1.77	4.52
3b	-6.36	-2.01	4.35
3c	-6.37	-2.04	4.33
3d	-6.34	-1.83	4.51
3e	-6.35	-1.99	4.36
3f	-6.27	-1.74	4.53
3g	-6.23	-1.53	4.7

known as the ionisation potential (I). The energy released when a proton is introduced to a system is known as electron affinity (A). It is connected to the E_{HOMO} and E_{LUMO} energies via the formula: $A=-E_{LUMO}$; $I = -E_{HOMO}$, when the values of I and A are known, the electronegativity (χ) and global hardness (η) may be calculated. The electronegativity of an atom or a group of atoms is defined as the ability of an atom or a group of atoms to draw electrons towards itself. It can be calculated using the following formula: $\chi = I + A/2$; $\eta = I - A/2$ Chemical softness ($^{\delta}$) refers to an atom's or a group of atoms' ability to accept electrons. It is calculated using the following formula: $^{\delta}=1/\eta$ .Electrophilicity index is a measure of energy loss due to maximum electron flow between donor and acceptor. The electrophilicity index (ω) calculated as follows. $\omega= \chi\ 2/2\eta$. The quantum chemical characteristics of 1,2,4 oxadiazole derivatives computed using Koopman's theorem equations[31-33] are shown in Table 5. Final products (3a-3g) are more reactive than starting compounds proved by low (ΔE) values in the range 4.3-4.7.

Molecular electrostatic potential map (MEP)

MEP was estimated using DFT/B3LYP at 6-311G (d,p) basis set for all compounds, and MEP surfaces are plotted in Fig. 3. The size, shape, charge density, and reactive sites of the molecules are surface mapped with an electrostatic potential surface [34-36]. The different values of the electrostatic potential represented by different colors; red represents the regions of the most negative electrostatic potential, blue represents the regions of the most positive electrostatic potential and green represents the region of zero potential [36]. Furthermore, the molecular electrostatic potential can be used to evaluate a compound's reactivity to electrophilic and nucleophilic attacks. Fig. 3 provides a visual representation of the chemically active sites andcomparative reactivity of atoms.

Mulliken charge analysis (MEP)

The Mulliken populations clearly provide the most straightforward representation of the charge distribution. The charge density function can be used to determine crucial molecule features such as the charges on the various atoms, the molecular dipole moment, and the electrostatic potential around the molecule. The Mulliken charges for the non-H atoms of the title chemical were estimated at the B3LYP level in gas phase using the 6-311G basis set. The atomic charges for the initial molecule revealed that C5, C8, and N7, O9 have the largest positive and negative charges, respectively. The intermediate, N7 O13 and N9, are the most negative, whilst C5, C8, are the most positive charge positions.On the other hand, it is evident that the final products have the most negative charges, with N7 and C21 and C8 and C9 having the most positively charged atoms. The most vulnerable places for nucleophilic assaults, or electron donation, are the positively charged centres. The most negatively charged centres, on the other hand, are the most vulnerable to electrophilic attack. The acquired findings are added together in Fig. 4 and Table 6.

Antibacterial activity

Using the agar diffusion method, all the compounds were tested for antibacterial activity against Gram positive (*S. aureus and B. subtilis*) and Gram negative (*E. coli and P. aeruginosa*) microorganisms. As a positive control, gentamycin was used. The radius of inhibition zones was used to measure the antibacterial activity of the test substances. The average diameter of inhibitory zones (mm) was measured and compared to that of the reference drug Gentamycin.The antibacterial activity screening findings are summarized in Table 7. According to the screening results, most of the compounds had modest to moderate antibacterial activity against specific strains.

Molecular docking studies

MurG is a key enzyme in peptidoglycan production that is found in practically every bacterial species, making it a promising target for new antibiotics. MurG (PDB 7b6k), on the other hand, is a model for glycosyl transferases found in the great majority of

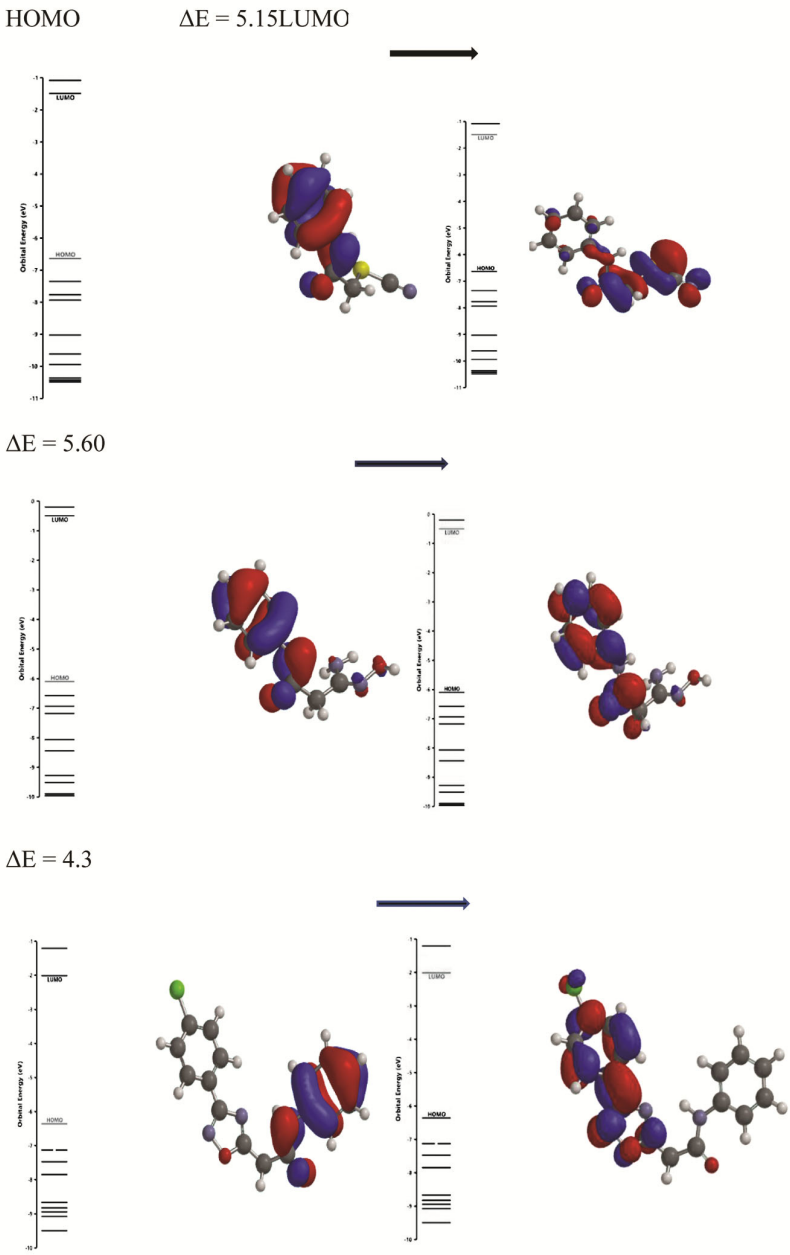

Fig. 2 — HOMO-LUMO plots for starting compound N-Phenyl-2-thiocyanato-acetamide, intermediate 2-(N-Hydroxycarbamimidoyl)-N-phenyl-acetamide and final compound 2-(3-Chloro-[1,2,4]oxadiazol-5-yl)-N-phenyl-acetamide

Table 5 — The quantum chemical characteristics of 1,2,4 oxadiazole derivatives

Ionisation potential $I = [-E_{HOMO}]$	Electron affinity $A = [-E_{LUMO}]$	Electronegativity $\chi=(I+A)/2$	Global hardness $\eta=(I-A)/2$	Softness $\delta=1/\eta$	Electrophilicity $\omega=\chi^2/2\eta$
6.64	1.49	4.065	2.575	0.3883	3.2085
6.1	0.5	3.3	2.8	0.3571	1.9446
6.29	1.77	4.03	2.26	0.4424	3.5931
6.36	2.01	4.185	2.175	0.4597	4.0262
6.37	2.04	4.205	2.165	0.4618	4.0836
6.34	1.83	4.085	2.255	0.4434	3.7000
6.35	1.99	4.17	2.18	0.4587	3.9882
6.27	1.74	4.005	2.265	0.4415	3.5408
6.23	1.53	3.88	2.35	0.4255	3.2030

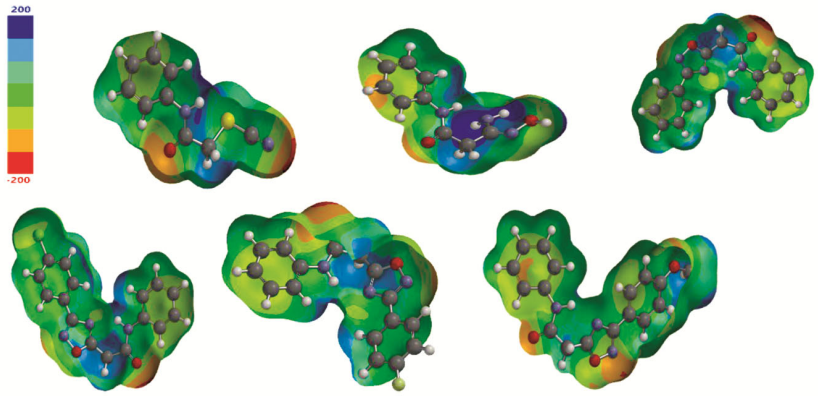

Fig. 3 — MEP plots of synthesis scheme of (3-Chloro-[1,2,4]oxadiazol-5-yl)-N-phenyl-acetamide(1-3)

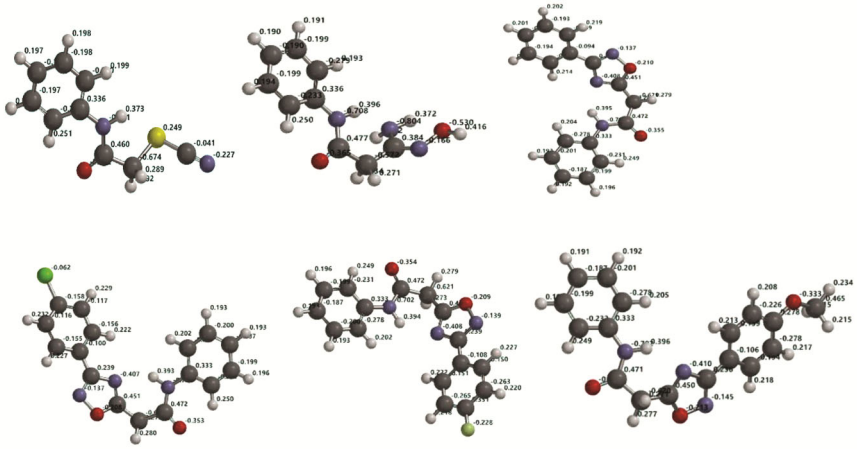

Fig. 4 — The DFT calculated Mulliken s atomic charges of synthesis of (3-Chloro-[1,2,4]oxadiazol-5-yl)-N-phenyl-acetamide(1-3)

Table 6 — Mulliken charge analysis for compounds in the synthesis scheme.

Stating compound (1)		Intermediate (2)		Products (3a-3g)	
Atom label	Mulliken charge	Atom label	Mulliken charge	Atom label	Mulliken charge
C1	-0.198	C1	-0.199	C1	-0.2
C2	-0.186	C2	-0.19	C2	-0.19
C3	-0.197	C3	-0.199	C3	-0.2
C4	-0.229	C4	-0.233	C4	-0.23
C5	**0.336**	**C5**	**0.336**	C5	0.333
C6	-0.27	C6	-0.279	C6	-0.28
C8	**0.46**	**C8**	**0.477**	**C8**	**0.472**
C10	**-0.674**	C11	0.384	**C9**	**0.451**
C12	-0.041	C14	-0.572	C12	0.236
N7	**-0.681**	**N7**	**-0.708**	C15	-0.09
N13	-0.227	**N9**	**-0.804**	C16	-0.16
O9	-0.342	N12	-0.166	C17	-0.19
S11	0.249	O10	-0.365	C18	-0.18
		O13	-0.53	C19	-0.19
				C20	-0.16
				C21	**-0.62**
				N7	**-0.7**
				N11	-0.41
				N13	-0.14
				O10	-0.36
				O14	-0.21

Table7 — The antibacterial activity screening findings of 1,2,4 oxadiazole derivatives

Compound		Zone of inhibition in diameter (mm)			
		B. subtilis	*S. aureus*	*P.aeruginosa*	*E. coli*
a	Phenyl	15	17	18	15
b	4-chlorophenyl	19	18	19	18
c	3-chlorophenyl	18	19	21	22
d	4-fluorophenyl	23	21	24	20
e	3-fluorophenyl	25	21	28	26
f	4-methoxyphenyl	21	19	26	15
g	3-methoxyphenyl	20	18	21	16
Gentamycin	-	35	30	36	35

Table 8 — Docking parameters via FLARE GUI

Name		LF Rank Score	LF dG	LF VSscore	LF LE	Binding interactions
Co-crystallized ligand		-5.907	-7.646	-8.088	-0.45	Tyr A 229, Phe A 204 pi-pi, Tyr A 221 HB
3a	Phenyl	-7.723	-9.007	-9.893	-0.409	Tyr A 229, Phe A 199 pi-pi,
3b	4-chlorophenyl	-6.712	-7.556	-8.581	-0.36	Tyr A 229, Phe A 204 pi-pi, Tyr A 221 HB
3c	3-chlorophenyl	-7.212	-8.51	-9.777	-0.387	Val A 203HB
3d	4-fluorophenyl	-9.941	-7.952	-9.154	-0.361	Tyr A 229, Phe A 204,Trp A 249 pi-pi
3e	3-fluorophenyl	-12.05	-7.735	-8.788	-0.352	Tyr A 229, Phe A 204,Trp A 249 pi-pi, Cys A234 Pi -sulphur
3f	4-methoxyphenyl	-6.554	-7.447	-8.506	-0.324	Tyr A 229, Phe A 204, Trp A 249 pi-pi,
3g	3-methoxyphenyl	-6.538	-8.189	-9.113	-0.356	Tyr A 229, Phe A 204, Trp A 229 pi-pi, Cys A234 Pi -sulphur

prokaryotic and eukaryotic cells[37].The docking results of possibly active synthesized derivatives of 2-(3-aryl-1,2,4-oxadiazol-5-yl)-n-phenylacetamide against glycosyl transferase protein were synchronized with *in-vitro* antimicrobial screening results.The docking analysis of tested compounds was performed through FLARE GUI software to predict the binding affinity of ligand and best orientation conformation of each compound[38]. Using FLARE extensions in python programming Ramachandran plots for the downloaded protein, specific low energy conformations for (phi) and (psi) or stable conformations of amino acid residues are discussed, as well as favorable and unfavorable locations for amino acid residues. (Fig. 5) Points on the plot indicate the ϕ (phi) and (psi), the torsion angles of amino acid residues in a 3D protein model. As demonstrated in Fig. S1 (Supplementary Information), all docked molecules had great binding to amino acids in the active pocket of the designated protein. The docked molecules (3a-3g) had better docking confirmation and a better LF score (-12.52 to -6.0) than the co-crystallized ligand. Furthermore, a molecular modelling analysis revealed that the most interactions of compounds (3a-3g) occur with amino acids Tyr A 229, Phe A 204, Trp A 249, and Tyr A 221in the binding pocket of the PDB 7b6k. Table 8 shows the results. The 3e derivative with fluorine in the meta position has the highest LF Rank score of all the synthesized derivatives.

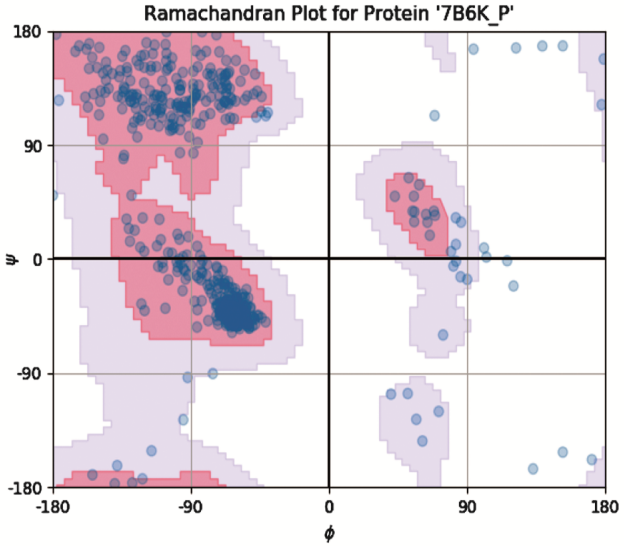

Fig. 5 — Ramachandran plot constructed by using Flare Gui extensions describing that whether amino acid residues reside in "accepted region" or "unaccepted" region. A better 3D protein modal should contain >90% amino acid residues in favored quadrant of Ramachandran Plot

Conclusion

For the synthesized derivatives of 2-(3-aryl-1,2,4-oxadiazol-5-yl)-n-phenylacetamide derivatives, the *In silco* screening predicted favorable pharmacokinetics and non-toxicity. The chemical reactivity was investigated using the estimated HOMO and LUMO energies. The MEP surface analysis map and the Mulliken population analysis map provide information on their reactive sites. The resulting compounds (3a-3g) were more polarizable than the beginning materials and had a high chemical reactivity and termed as "soft molecules." A variety of novel 1,2,4-disubstituted Oxadiazole derivatives were investigated for antibacterial activity. 3d and 3e analogs, among the produced compounds, had exceptional antibacterial activity against the microorganisms tested. In silico molecular docking studies were also linked to in vitro antibacterial activity of examined compounds.The phenyl ring substituted with an electron-withdrawing group like fluorine (3d & 3e) demonstrated higher biological activity due to a change in lipophilicity, according to the results of molecular docking. As a result of the foregoing findings, it can be stated that the current 1,2,4-oxadiazole study has the potential to serve as new pharmacophores for the development of new antibiotics.

Supplementary Information

Supplementary information is available in the website http://nopr.niscpr.res.in/handle/123456789/58776.

Acknowledgment

The authors are thankful to the Department of Chemistry, St. Francis College for Women for providing software like Flare V4 Cresset U.K. The authors extend their appreciation to *Neotel Systems & Services*, Chandigarh, India for their support.

References

1 Bostrom J, Hogner A, Llinas A, Wellner E & Plowright A T, *J Med Chem,* 55 (2012) 1817.
2 Gobec M, Toma T & Markovi_C T, *Chem-Biol Interact*, 240 (2015) 200.
3 Filho J M D S, Lima J G D & Leite L F C C, *J Heterocyclic Chem*, 46 (2009) 722.
4 Leite L F C C, Ramos M N & Silva J B P D, *Il Farmaco,* 54 (1999) 747.
5 Kayukova L A, Praliev K D & Akhelova A L, *Pharm Chem J*, 45 (2011) 468.
6 Shaikh A & Meshram J, *J Heterocyclic Chem,* 53 (2016) 1176.
7 Guda D R, Park S J & Lee M W, *Eur J Med Chem,* 62 (2013) 84.
8 Wang M, Liu T & Chen S, *Eur J Med Chem*, 209 (2021) 112874.
9 Palumbo Piccionello A, Musumeci R & Cocuzza C, *Eur J Med Chem,* 50 (2012) 441.
10 Rai N P, Narayanaswamy V K, Govender T & Manuprasad B K, *Eur J Med Chem,* 45 (2010) 2677.
11 Kumar D, Patel G & Chavers A K, *Eur J Med Chem*, 46 (2011) 3085.
12 Zhang H Z, Kasibhatla S & Kuemmerle J, *J Med Chem*, 48 (2005) 5215.
13 Vaidya A, Jain S, Kumar B P, Singh S K, Kashaw S K & Agrawal R K, *Monatsheftef€ur Chemie – Chem Mon,* 151 (2020) 385.
14 Lankau H-J, Unverferth K & Grunwald C, *Eur J Med Chem,* 42 (2007) 873.
15 Mohammadi-Khanaposhtani M, Ahangar N & Sobhani S, *Bioorg Chem*, 89 (2019) 102989.
16 Ergun Y, Orhan O F, Ozer U G & Gisi G, *Eur J Pharmacol,* 630 (2010) 74.
17 Sangshetti J N & Shinde D B, *Eur J Med Chem,* 46 (2011) 1040.
18 Abulwerdi F A, Shortridge M D & Sztuba-Solinska J, *J Med Chem,*59 (2016) 11148.
19 Filho J M D S, Silva D M A D Q E, Macedo T S, Teixeira H M P & Soares M B P, *Bioorg Med Chem,* 24 (2016) 5693.
20 Deb P K, Al-Shar'I N A, Venugopala K N, Pillay M & Borah P, *J EnzymInhib Med Ch,* 36 (2021) 869.
21 Srivani K, Thirupathaiah T, Laxminarayana E & Thirumala C M, *Rasayan J. Chem,* 11 (2018) 1004.
22 Gece G, *Corros Sci*, 50 (2008) 2981.
23 Lewis D F V, Ioannides C & Parke D V, *Xenobiotica,* 24 (1994) 401.
24 Sudeepa K, Narsimha N, Aparna B, Sreekanth S, Aparna A V, Ravi M, Mohmed J & Devi C S*, J Chem Sci,* 130 (2018) 52.
25 Singhal S, Khanna P & Khanna L, *Heliyon,* 5 (2019) 1.
26 Kwong E, *Oral Formulation Roadmap from Early Drug Discovery to Development*, (John Wiley & Sons, Canada), 2017 pp 272.
27 Parr R G & Yang W, *Density-functional theory of atoms and molecules*, (Oxford University Press, New York) 1989, pp 333.
28 Uesugi Y, Mizuno M, Shimojima A & Takahashi H, *J Phys Chem*, 101 (1997) 268.
29 Padmaja L, Kumar C R, Sajan D, Joe I H, Jayakumar V & Pettit G R, *J Raman Spectrosc*, 40 (2009) 419.
30 Sudha S, Sundaraganesan N, Kurt M, Cinar M & Karabacak M, *J Mol Struc,* 985 (2011)148.
31 Koopmans T, *Physica,* 1 (1993) 104.
32 Ayers P & Parr R G*, J Am Chem Soc*, 122 (2000) 2010.
33 Xavier S, Periandy S & Ramalingam S, *Spectrochim Acta Part A,* 137 (2015) 306.
34 Alorta I & Perez J J, *Int J Quant Chem*, 57 (1996) 123.
35 Luque F J, Orozco M, Bhadane P K, Gadre S R, *J Phys Chem*, 97 (1993) 9380.
36 Bendjeddou A, Abbaz T, Gouasmia A K & Villemin D, *Int Res J Pure Appl Chem*,12 (2016) 1.
37 Yao Liu & Eefjan Breukink, *Antibiotics,* 5 (2016) 28.
38 Hooft R W W, Sander C & Vriend G, *CABIOS,* 13 (1997) 425.